Article ID: 1001-3555(2014)03-0259-09

Reaction Mechanism of Acetylene Hydrochlorination in Cu-based Catalyst

ZHAO Pu-jun[1], WANG Fu-min[1], CAI Wang-feng[1], ZHANG Jin-li[1], ZHANG Xu-bin[1,*]
(*College of Chemical Engineering*, *Tianjin University*, *Tianjin* 300072, *China*)

Abstract: The reaction mechanism of acetylene hydrochlorination in Cu-based catalyst was studied using the density functional theory (DFT). Two possible paths for acetylene hydrochlorination reaction in Cu-based catalyst were illustrated with corresponding transition states. We applied the reaction mechanism to various metal chlorides and obtained an order of different catalysts by analyzing the activation free energies and reaction rate constants. The result was compared with experimental ones to verify the reaction mechanism. The deactivation reason of Cu-based catalyst and the reaction on the N/P-doped graphene were also discussed. The conclusions derived from this study would shed light on the experimental design of novel non-mercury catalyst with high performance.

Key words: acetylene hydrochlorination; Cu-based catalyst; DFT; Reaction mechanism; N/P doping
CLC number: O643.32 **Document code**: A

The preparation of vinyl chloride monomer (VCM) is the foundation for polyvinyl chloride (PVC). The main process of production of VCM includes oxychlorination of ethylene, oxychlorination of ethane and acetylene hydrochlorination. Acetylene hydrochlorination has been the most widely used process for the production of VCM and will be the main process in the near future because of the situation of resources in China. In acetylene hydrochlorination, the $HgCl_2$/Carbon was used as the catalyst, which may cause mercury pollution on the environment and its sustainable development has been severely constrained. It is crucial to explore environmentally friendly non-mercury catalysts for acetylene hydrochlorination for sustainable PVC production via the acetylene-based method in China.

In 1975, Kiyonori[1] studied the catalytic activity of nearly 20 kinds of supported metal chlorides for acetylene hydrochlorination. He proposed that the reaction conversion was related to the electron affinities of the cation in metal chloride. According to his studies, Pd^{2+}, Hg^{2+}, Cu^{2+}, Cu^{+} and Ag^{+} have better catalytic activity and the order followed as $Pd^{2+}>Hg^{2+}>Cu^{2+}>Cu^{+}>Ag^{+}$.

In 1985, Hutchings and co-workers[2-5] found that the catalytic activity of the metal complex correlated with the standard electrode potential of the metal cations. They predicted that Au^{3+} might have high catalytic activity and this was confirmed by their experimental studies. Nkosi[6-7] dissolved chloroauric acid in aqua regia, and got effective Au catalyst with wet impregnation method.

Moreover, Pd^{2+} catalyst[8] has drawn more attention from researchers and it also performed high catalytic activity for acetylene hydrochlorination. Strebelle[9] and Song[10] studied the catalytic activity of Pd^{2+} in detail and found that the initial activity of Pd^{2+} catalyst was high but was not stable and its activity was easily lost during the reaction.

Besides Au^{3+} and Pd^{2+}, Cu^{2+}[11], Pt^{2+}[12],

Received date: 2014-01-24; **Revised date**: 2014-03-28.
Foundation: The project was supported by the National Basic Research Program of China (973 Program) (Grant No: 2012CB720302).
First author: Zhao Pujun (1988-), male, master.
* **Corresponding author**: E-mail: tjuxb@tju.edu.cn; Tel: 022-27890041.

Pt^{4+}[13], Rh^{3+}[14], Ir^{3+}[15], Ru^{3+}[14-15] also have been tested to show high catalytic activity for acetylene hydrochlorination. Among the metal cations tested, some noble metals were proved to exhibit good catalytic activity, but considering their high cost and easy deactivation, they may not be the possible candidate to take the place of commercial $HgCl_2$/carbon.

Among the non-noble metal catalysts, Cu-based catalyst was proved to show good catalytic activity for acetylene hydrochlorination and its high stability was also testified. Wang[11] reported a Au^{3+}-Cu^{2+}/C catalyst with a stability exceeding 200 h on stream, the conversion and selectivity can reach 99.5%. Compared with $HgCl_2$ catalyst, $CuCl_2$ catalyst exhibit lower activity but better stability. Deng[16] found that $SnCl_2$ show high catalytic activity, they reported a $SnCl_2$-$BiCl_3$-$CuCl_2$ catalyst but its life span was not long enough because $SnCl_2$ lost easily. Jiang[17] claimed they developed a catalyst complex, involving noble metal chlorides such as $PtCl_2$, $PdCl_2$, $AuCl_3$ and base metal chlorides like $CuCl_2$, $BiCl_2$, the proportion of precious metal and base metal was 1∶2-3. The conversion can reach 97% ~99% and the selectivity was 99% at 110 ℃.

With the rapid development of computer technology, various of software and devices updated quickly, it was possible to simulate a complex system by using quantum chemistry theories and methods[18-19], which had been important means to explore the link between microstructure and macroscopic properties. Conte[20] simulated the reaction mechanism of acetylene hydrochlorination on $AuCl_3$ catalyst, he found that the C_2H_2 is prior to adsorbing on catalyst than HCl. Mitchenko[12-13] expounded the catalytic mechanism of acetylene hydrochlorination on K_2PtCl_6 that Pt(Ⅱ) and intermediate Pt(Ⅳ) played a complementary role in the reaction.

In this work, a systemic study of the catalytic mechanism of Cu-based catalyst for acetylene hydrochlorination on the graphene was carried out in DFT[21-22]. The reaction rate constants of different reactions were obtained. Since the reaction mechanism of $CuCl_2$ and CuCl is similar, we only illustrate $CuCl_2$ catalyst.

1 Computational methods

All calculation was carried out with the Dmol3 module of Materials Studio. The geometrical optimizations with the population analysis of the reactants, products, intermediates and transition states were performed by using BLYP function[23-24], together with the DND basis set. The all electron relativistic core treat method was implemented for relativistic effects. A smearing of 0.005 Ha (1 Ha = 27.21 eV) to the orbital occupation was applied to achieve accurate electronic convergence. Vibrational analysis was done for some structures to determine whether the steady state is a lower energy point or a transition state.

2 Results and discussion

2.1 The adsorption of acetylene and hydrogen chloride on $CuCl_2$ catalyst

For $CuCl_2$ molecule, the linear structure is the most stable one. The bond length of Cu-Cl is 2.100 Å, the angle of Cl-Cu-Cl is 180°. The lowest unoccupied molecular orbital (LUMO) of this structure exhibits a large lobe on the active center Cu and two small ones on the two side chlorines (shown in Fig. 1). It is easy for Cu^{2+} to get electron from and adsorb with reactant. And Cl^- is also a possible adsorption site.

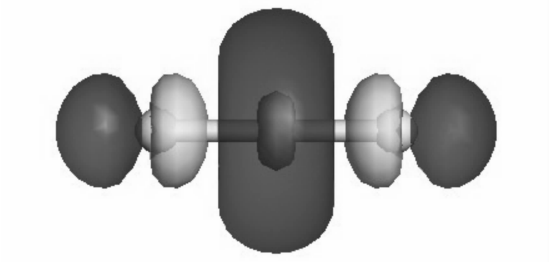

Fig. 1 The calculated LUMO state for $CuCl_2$ at the BLYP level

The possible way of the adsorption of acetylene and hydrogen chloride on Cu-based catalyst is calculated and shown in Fig. 2. E_{ad} shown in the figure represents the adsorption energy between the reactants and the catalyst. It is calculated by using equation (1).

$$E_{ad} = E_{\text{absorption-state}} - (E_{\text{reactant}} + E_{\text{catalyst}}) \quad (1)$$

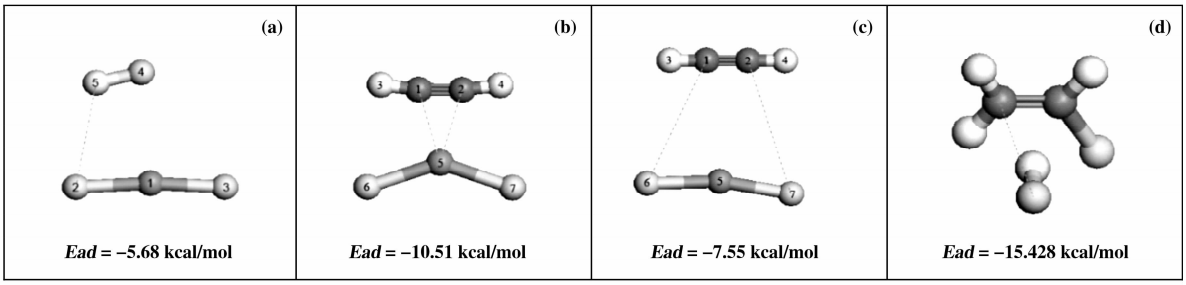

Fig. 2 The adsorption structures in the reaction

Our results showed that there are three different ways for the reactant adsorbing on the catalyst. The hydrogen chloride adsorbs on the $CuCl_2$ catalyst mainly by hydrogen bonding, and the adsorption energy is 5.68 kcal · mol^{-1} (shown in Fig. 2 (a)). The Cl 4-H 5 bond is slightly weakened and stretched from 1.302 Å to 1.306 Å, the distance between Cl 2 and H 5 is 2.875 Å. The acetylene adsorbs on the $CuCl_2$ catalyst by forming a coordination structure via C≡C bond of C_2H_2 and Cu 5 (shown in Fig. 2 (b)). We analyzed the Mulliken charge and found that the electric charge of C 1 and C 2 range from −0.151 e to −0.135 e while Cu 5 is from +0.371 e to +0.309 e, indicating the π electron of C_2H_2 transfer to Cu 5, thus the C≡C bond is weakened and stretched from 1.205 Å to 1.223 Å, the distance between C 2 and Cu 5 is 2.245 Å, some negative charge transfer to Cl 6 and Cl 7, which change from −0.187 e to −0.281 e, the polarity of Cu-Cl bond is enhanced and the bond stretches from 2.100 Å to 2.171 Å, the linear structure of $CuCl_2$ is bended and made a 140.77° angle, the adsorption energy is 10.51 kcal · mol^{-1}. Besides, we considered a situation that the acetylene adsorbs on the catalyst in a metastable state (shown in Fig. 2 (c)). The electron density of the C≡C is enhanced, the electric charge of C 1 and C 2 range from −0.151 e to −0.202 e, the positive charge transfer to H 3 and H 4, which vary from +0.151e to +0.227 e, the electric charge of Cl 6 and Cl 7 stay the same, the distance between C 2 and Cl 7 is 4.232 Å, the linear structure of $CuCl_2$ is bended and made a 167.51°angle, the adsorption energy is 7.55 kcal · mol^{-1}. Comparing the adsorption energy, we drew a conclusion that the acetylene is prior to adsorbing on the $CuCl_2$ catalyst than hydrogen chloride. Furthermore, the hydrogen chloride adsorbs on the vinyl chloride by hydrogen bonding (shown in Fig. 2 (d)), the adsorption energy is 15.428 kcal · mol^{-1}, it is possible to generate dichloroethane.

2.2 Reaction mechanisms of acetylene hydrochlorination over $CuCl_2$ catalyst

The reaction mechanism of acetylene hydrochlorination catalyzed by $CuCl_2$ was systematically studied. The reaction paths beginning with the adsorbed structure on $CuCl_2$ catalyst (shown in Fig. 2 (b, c)) are donated as path 1 and path 2. The reaction mechanism of these paths will be further discussed below.

2.2.1 Reaction mechanism of path 1　The reaction path 1 is shown in Fig. 3 and Fig. 4. The two C atoms of C_2H_2 and Cu 5 atom form a compound structure via a π-σ coordination bond. The π electron of C_2H_2 transfers to the unoccupied molecular orbital of Cu^{2+}, thus the C ≡ C bond is weaken and stretched from 1.205 Å to 1.223 Å. The C 2 atom (−0.135 e) from C_2H_2 and Cu 5 atom (+0.309 e) begin to interact with each other and their distance is shorten from 2.244 Å to 2.015 Å in $R_{1\text{-}1}$ and $TS_{1\text{-}1}$. Thus, a four-membered ring is formed in $TS_{1\text{-}1}$, the π electron on the Cu 5 transfers back to C_2H_2 through the four-membered ring. Meanwhile, the electronegativity of the Cl 6 atom (−0.203 e) is high, so the negative charge on the C 1 atom reduces from −0.135 e to −0.045 e while the one on the C 2 atom enriches from −0.135 e to −0.277 e. There is no significant change in the electron of the Cu 5 atom (+0.313 e). A nucleophilic addition reaction is finished with producing the intermediate chlorovinyl $P_{1\text{-}1}$. In the intermediate $P_{1\text{-}1}$, the Cu catalyst becomes

a CuCl coordinate structure by losing a Cl atom, but it still maintains its planar structure due to the adsorption of chlorovinyl. The TS_{1-1} transition state requires an activation free energy of 13.444 kcal · mol^{-1}, and a 6.791 kcal · mol^{-1} free energy is absorbed during this reaction.

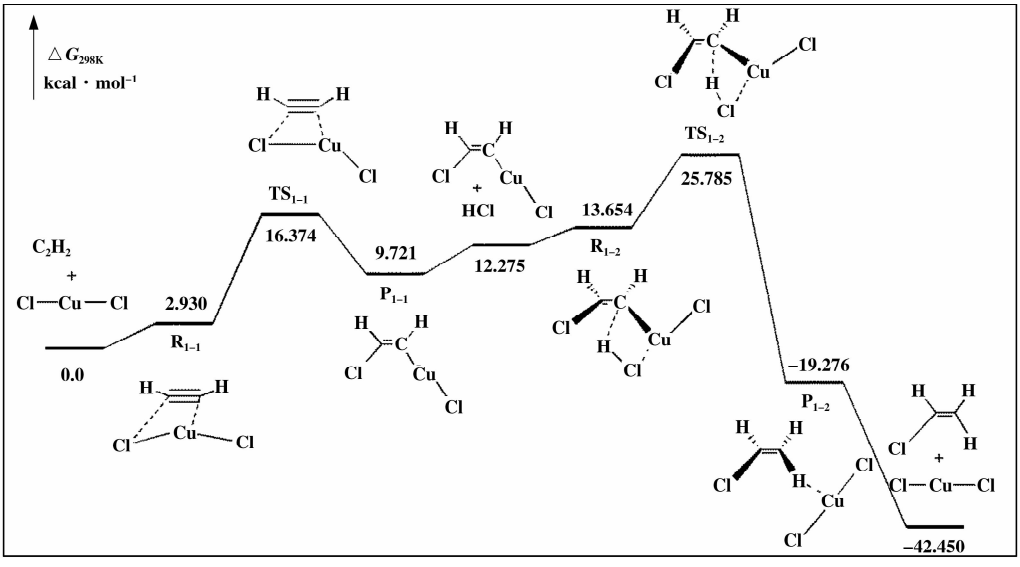

Fig. 3 DFT calculated energy surface for C_2H_2 hydrochlorination through path 1

When the intermediate P_{1-1} adsorbs HCl on the Cu 5 site, they will generate product P_{1-2} with a transition state TS_{1-2}. In TS_{1-2}, the C 2-Cu 5 bond is broken due to the adsorption of HCl. The Cl of the adsorbed HCl bonds with Cu 5 and the bond length is 2.408 Å. The H 9 atom (+0.339 e) from HCl adsorbs with the C=C bond by hydrogen bonding. An electrophilic attack occurs between the H 9 atom (+0.348 e) and the C 2 atom (−0.371 e), while their distance is shorten from 3.047 Å to 1.658 Å in R_{1-2} and TS_{1-2}. In TS_{1-2}, the negative electron transfers from the Cu 5 atom to the C 2 atom (−0.447 e), and the Cu 5 atom (+0.330 e) adsorbs with the Cl 8 atom (−0.223 e) so a four-membered ring is formed. The TS_{1-2} transition state requires an activation free energy of 12.131 kcal · mol^{-1}, and a 32.921 kcal · mol^{-1} free energy is released during this reaction. In the final product P_{1-2}, the chloride ethylene desorbs from the $CuCl_2$ with 23.174 kcal · mol^{-1} free energy released, and the $CuCl_2$ catalyst recovers to the linear structure.

Besides, if the HCl in the gas phase could adsorb on the C 2 and Cu 5 site efficiently, the second step of path 1 would be easy. In this case, chlorovinyl is not hard to be desorbed from the catalyst as the desorption energy is as low as 9.75 kcal · mol^{-1}, which can't cause the catalytic activity of $CuCl_2$ to decrease due to the active Cu site being occupied. Therefore, the second step of path 1 can proceed successfully as long as the HCl is supplied sufficiently. In addition, we analyzed the adsorption energy of graphene and each structure in path 1 and found that the adsorption energy of graphene and P_{1-1} is 3.253 kcal · mol^{-1}, which is the least of all. We deduced that the intermediate chlorovinyl P_{1-1} can be desorbed from the carrier, which leads to the deactivation of catalyst.

2.2.2 Reaction mechanism of path 2 The reaction path 2 is shown in Fig. 5 and Fig. 6. The Cl 6 and Cl 7atoms from HCl adsorb with the C≡C bond. A nucleophilic attack occurs between the Cl 6 atom (−0.187 e) and the C 2 atom (−0.202 e), while their distance is shorten from 3.852 Å to 2.091 Å in R_2 and TS_2. Thus the C≡C bond is weakened as the decrease of the electron density. The C 1(2) atom from C_2H_2 and Cl 6(7) atom begin to interact with each other. In TS_2, the bond of Cu 5-Cl 6 stretches from 2.111 to 2.659 Å and rotates upward to form an angle of 84.838°. The conformation of transition state TS_2 through R_2 needs an activation free energy of 53.058 kcal · mol^{-1},

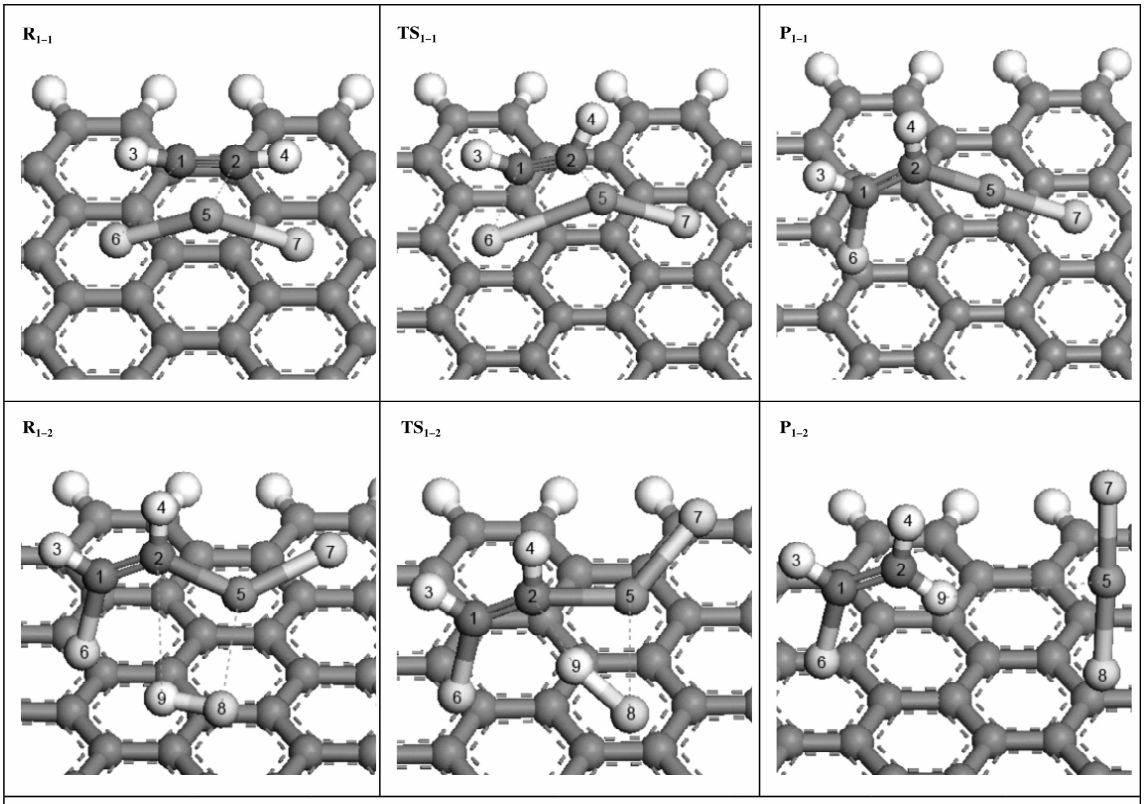

Atom-Bond	R_{1-1}	TS_{1-1}	P_{1-1}	Atom-Bond	R_{1-2}	TS_{1-2}	P_{1-2}
1-2	1.223	1.270	1.357	1-2	1.327	1.341	1.338
2-5	2.244	2.015	1.888	2-9	3.047	1.658	1.090
5-6	2.171	2.344	3.494	9-8	1.342	1.491	3.885
6-1	3.226	2.249	1.755	8-5	2.497	2.408	2.103
1-5	2.245	2.568	2.932	5-2	1.937	1.998	4.420

Fig. 4 Optimized key structures for C_2H_2 hydrochlorination through path 1 (the unit of bond length is Å)

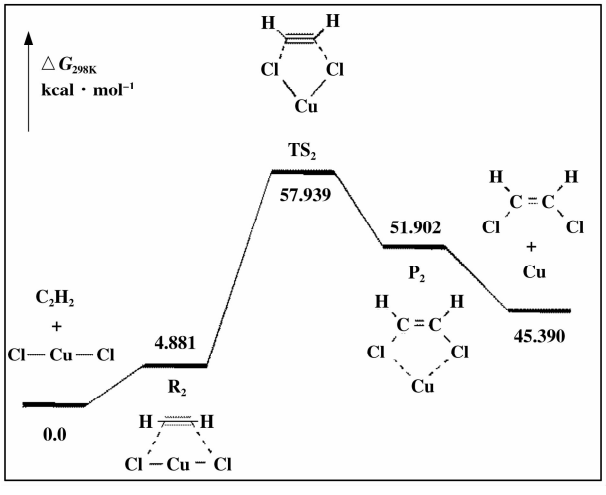

Fig. 5 DFT calculated energy surface for C_2H_2 hydrochlorination through path 2

and 47.021 kcal · mol^{-1} free energy is absorbed during the reaction process. In P_2, the linear structure of the $CuCl_2$ catalyst is broken and Cu is generated, so the catalyst lost its activity. As the energy barrier of the positive reaction is much larger than the reverse reaction, the reaction is hard to proceed.

2.3 Verification of reaction mechanism by dynamic analysis

According to transition state theory (TST), the reaction rate constant is related with the activation free energy. It could be calculated by equation 2[25-26].

$$k = A exp(^{-\Delta}G/RT) \quad (2)$$

Where $^{-\Delta}G$ is the activation free energy, which is the free energy between the transition state and reactant,

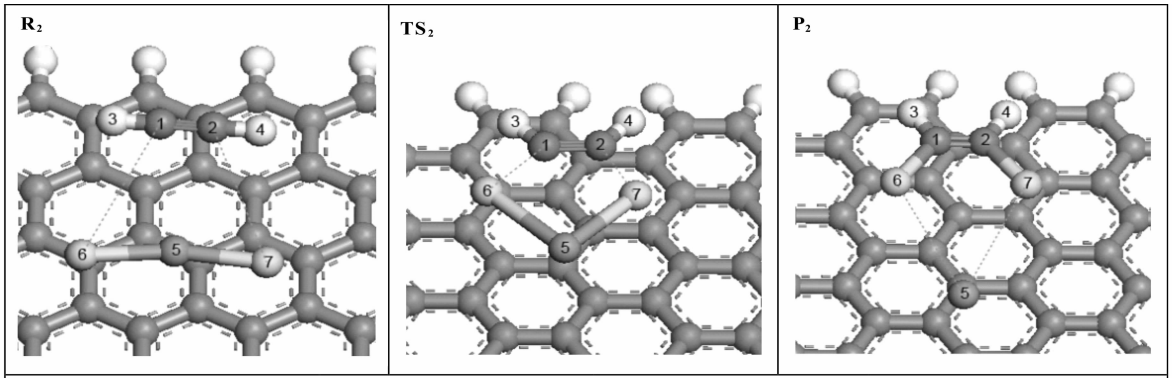

Atom-Bond	R_2	TS_2	P_2
1-2	1.210	1.307	1.173
1-6	3.852	2.091	1.745
6-5	2.111	2.659	4.256
5-7	2.110	2.486	4.232
7-2	3.905	1.941	1.745

Fig. 6 Optimized key structures for C_2H_2 hydrochlorination through path 2 (the unit of bond length is Å)

R is ideal gas constant, T is the reaction temperature, and A represents the pre-exponential factor, which is calculated by equation 3.

$$A = \Pi_{i=1}^{3N} V_i / \Pi_{i=1}^{3N-1} V_i' \quad (3)$$

Where V_i, V_i' are the frequency of the reactant and the transition state.

The values of A for paths 1-1, 1-2 and 2 are 1.08×10^5, 7.39×10^5 and 1.07, respectively. The rate constants of path 2 are much lower than the other paths because of the high activation free energy and low value of A, indicating that the side reaction can't happen. To verify the reaction mechanism of path 1, we applied it to various metal chlorides and obtained an order of different catalysts by analyzing the activation free energies and reaction rate constants (shown in Fig. 7).

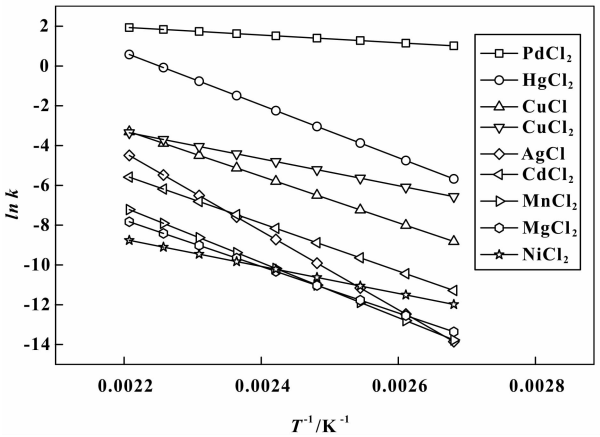

Fig. 7 Reaction rate constants versus the reaction temperature via TST calculation

The results showed that the relationship between $ln\ k$ and T^{-1} is linear, and the slope of the line reflects the activation free energy of each metal chloride. The temperature has more effect on which needs larger activation free energy such as Hg^{2+}, Ag^+ and Cu^+. When $T^{-1} = 0.0022\ K^{-1}$ ($T = 453\ K$), it is obvious that Pd^{2+}, Hg^{2+}, Cu^{2+}, Cu^+ and Ag^+ have higher rate constants and the sequence is followed as $Pd^{2+} > Hg^{2+} > Cu^+ > Cu^{2+} > Ag^+$, nearly same as the experimental result[1] obtained by predecessors, which means that the reaction mechanism is reasonable. Besides, considering the high adsorption energy between the vinyl chloride and hydrogen chloride, we also discussed the possibility of the consecutive reaction, which is an addition reaction of vinyl chloride with hydrogen chloride. We simulated the reaction path which needs an activation free energy of 41.538 kcal · mol^{-1}, much larger than the others. And the selectivity of the main reaction would drop to less than 99% if the reaction temperature rise to more than 200℃, which was consistent with our experiment. The experimental apparatus used

for acetylene hydrochlorination was identical with which described in reference[27]. The experiment was conducted under this reaction condition (n(HCl)/n(C_2H_2) = 1.1 : 1, 0.1 MPa, GHSV (C_2H_2) = 180 h^{-1}, 12% $CuCl_2$). We chose gas chromatograph (3420A) to detect the content of each component. The results showed that the selectivity was better at 140 ℃ (99.9%) than those at higher temperature (shown in Fig. 8).

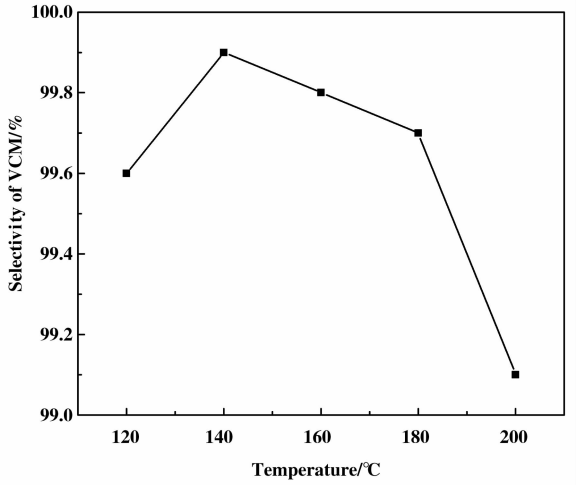

Fig. 8 Influence of temperature on selectivity

2.4 Influence of N/P doping

When C-based materials, such as activated carbon, graphene and carbon nanotubes, doped with N, B and P[28], their electronic property can be changed. Xu[29] found that the Au-based catalyst, which was supported by nitrogen doped graphene, showed better activity and stability than the one which carried by pure graphene. For nitrogen doped graphene, the structure become more stable because the negative charge gathered on the N atom (−0.502 e) and the C-N (1.421 Å) bond is shorter than C-C (1.430 Å), the Mulliken bond order of C-N (0.7248) is lower than C-C (0.9440), which means the polarity of C-N is larger than C-C, so the C-N bond is stronger than C-C. And the binding energy of pure graphene is 11.48 eV while N-graphene is 11.51 eV, which means N-graphene is more stable. Besides, the adsorption energy between the catalyst and graphene is amplified after doped with N or P. We still focused on the metal cations such as Pd^{2+}, Hg^{2+}, Cu^{2+} and Cu^{+}, studied the reaction rate constants on nitrogen or phosphorus doped graphene (shown in Fig. 9). The results showed that the reaction rate constants increased on nitrogen or phosphorus. doped

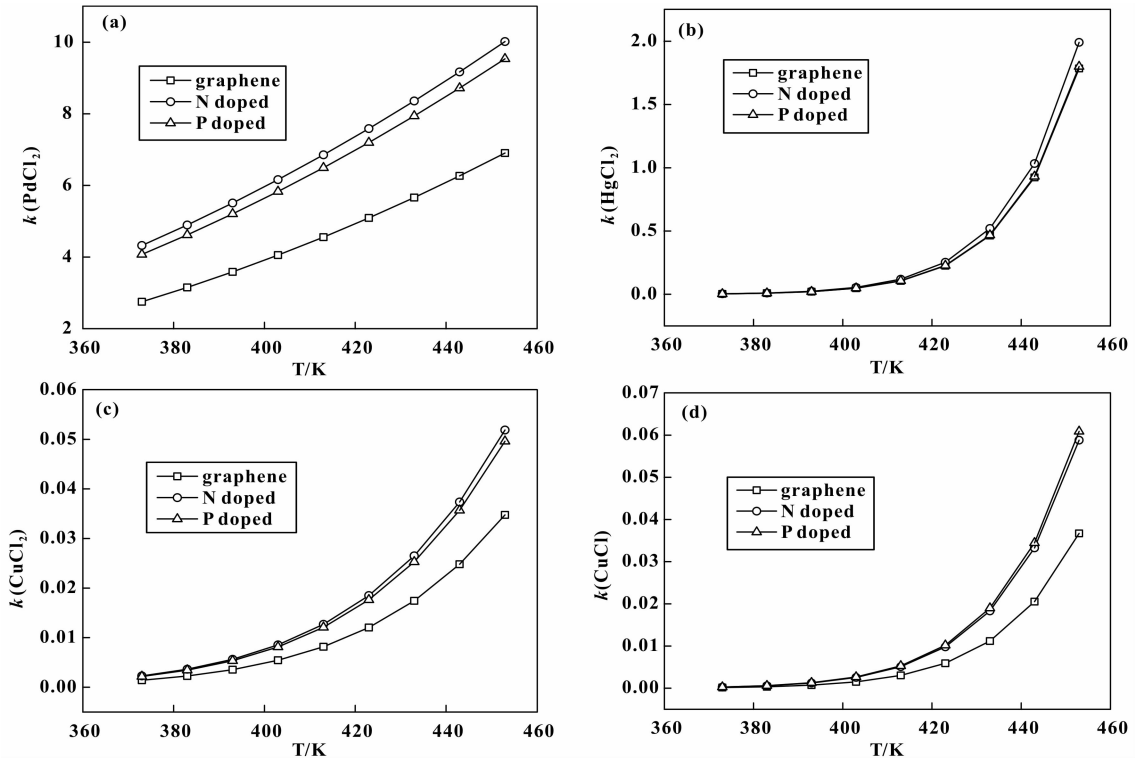

Fig. 9 Influence of doping N or P on reaction rate constants

graphene. The improvement depends on the metal cations, it would be considerable for some noble metal chlorides such as $PdCl_2$ but not effective to some base metal chlorides, for $HgCl_2$, it is useless to dope phosphorus on graphene (shown in (b)). For Cu-based catalyst, doping nitrogen is more suitable for $CuCl_2$ while phosphorus is better for CuCl (shown in (c, d)), but the reaction rate constants are still far less than the noble metal chlorides.

In order to explain the result, we analyzed the Mulliken charges of catalyst and found that the negative charge of graphene transfers to the catalyst, the atomic charge of the metal cations is reduced and the electron density of chlorine atom is enhanced, which is beneficial for the interaction of reactant and catalyst. For the reaction catalyzed by $CuCl_2$ on nitrogen doped graphene, the positive charge on the Cu atom is lessen from +0.813e to +0.453e, the negative charge on the Cl atom is increased from -0.441e to -0.536e. In addition, the Mulliken bond order is reduced from 0.905 to 0.590 and the bond stretches from 2.126 Å to 2.129 Å, indicating that the polarity of Cu-Cl is enhanced with the action of the N atom. Moreover, we calculated the activation free energy, it is dropped from 13.44 kcal · mol^{-1} to 13.08 kcal · mol^{-1}, which means the activation free energy can also be influenced by N/P doping. The adsorption energy of P_{1-1} and nitrogen doped graphene is 6.656 kcal · mol^{-1}, larger than the one before doping N. So the catalyst can stably adsorb on nitrogen or phosphorus doped graphene and it can enhance the dispersity and stability of catalyst and improve the catalytic activity.

3 Conclusions

In this work, we performed the density functional theory calculations to study the reaction mechanism of the acetylene hydrochlorination. The results showed that there are two paths for the acetylene hydrochlorination reaction catalyzed by $CuCl_2$ catalyst. We calculated the reaction rate constants of some other metal chlorides and obtained an order to verify the reaction mechanism, we drew a conclusion that Pd^{2+}, Hg^{2+}, Cu^{2+}, Cu^{+} and Ag^{+} show higher rate constants and the sequence is followed as $Pd^{2+} > Hg^{2+} > Cu^{+} > Cu^{2+} > Ag^{+}$, agreed with the experimental ones. In the deactivation mechanism discussed above, desorption of the intermediate chlorovinyl causes the decrease in acetylene conversion, and the element copper can't be generated due to their high energy barrier. Besides, the consecutive reaction which produce dichloroethane can't happen unless the reaction temperature is above 200 ℃. Furthermore, we studied the influence of nitrogen or phosphorus doped graphene. The negative charge gather on the N/P atom and the adsorption energy of catalyst and graphene is enhanced, which improve the stability of catalyst. The electron is diverted from graphene to the Cl atom of catalyst, the polarity of M-Cl is enhanced and the activation free energy can be reduced on nitrogen or phosphorus doped graphene. The improvement of rate constants is more effective for noble metal chlorides.

References:

[1] Kiyonori S. The vapor phase hydrochlorination of acetylene over metal chloride supported on activated carbon [J]. *Catal Lett*, 1975, **3**: 219-220.

[2] Hutchings G J. Vapor phase hydrochlorination of acetylene: correlation of catalytic activity of supported metal chloride catalysts [J]. *J Catal*, 1985, **96**: 292-295.

[3] Conte M, Carley A F, Hutchings G J. Reactivation of a carbon-supported gold catalyst for the hydrochlorination of acetylene [J]. *Catal Lett*, 2008, **124**(3/4): 165-167.

[4] Hutchings G J, Haruta M. A golden age of catalysis: a perspective [J]. *Appl Catal A*, 2005, **291**: 2-5.

[5] Hutchings G J. Reactions of alkynes using heterogeneous and homogeneous cationic gold catalysts [J]. *Top Catal*, 2008, **48**: 55-59.

[6] Nkosi B, Conville N J, Hutchings G J. Reactivation of a supported gold catalyst for acetylene hydrochlorination [J]. *J Chem Soc Chem Commun*, 1988, **1**: 71-72.

[7] Nkosi B, Conville N J, Hutchings G J, *et al*. Hydrochlorination of cetylene using gold catalysts : a study of catalyst reactivation [J]. *J Catal*, 1991, **128**: 378-386.

[8] Wang Sheng-jie(王声洁), Shen Ben-xian(沈本贤), Zhao Ji-gang(赵基钢), *et al*. Deactivation of $PdCl_2$/C catalyst in hydrochlorination of acetylene(乙炔氢氯化 $PdCl_2$/C 催化剂失活原因分析) [J]. *Petrochem Technol*(石油化工), 2009, **38**: 249-254.

[9] Strebelle, M. US [P] 5254777, 1993.

[10] Song Q L, Wang S J, Shen B X. Palladium-based catalysts for the hydrochlorination of acetylene: reasons for deactivation and Its regeneration [J]. *Petrol Sci Technol*, 2010, **28**: 1825-1833.

[11] Wang S J, Shen B X, Song Q L. Kinetics of acetylene hydrochlorination over bimetallic Au-Cu/C catalyst [J]. *Catal Lett*, 2010, **134**: 102-109.

[12] Mitchenko S A, Krasnyakova T V, Mitchenko R S, *et al*. Acetylene catalytic hydrochlorination over powder catalyst prepared by pre-milling of K_2PtCl_4 salt [J]. *J Mol Catal A Chem*, 2007, **275**: 101-108.

[13] Mitchenko S A, Krasnyakova T V, Mitchenko R S, *et al*. Catalytic hydrochlorination of acetylene by gaseous HCl on the surface of mechanically preactivated $K_2Pt_2Cl_6$ salt [J]. *J Mol Catal A Chem*, 2004, **212**: 345-352.

[14] Nkosi B, Conville N J, Hutchings G J. Vapour phase hydrochlorination of acetylene with group viii and IB metal chloride catalysis [J]. *J Catal*, 1988, **43**: 33-39.

[15] Conte M, Carley A F, Attard G, Herzing, *et al*. Hydrochlorination of acetylene using supported bimetallic Au-based catalysts [J]. *J Catal*, 2008, **257**: 190-198.

[16] Deng Guo-cai(邓国才), Wu Ben-xiang(吴本湘), Li Tong-shu(李同树), *et al*. 乙炔法合成氯乙烯固相非汞催化剂的研制[J]. *PVC*(聚氯乙烯), 1994, **6**: 5-9.

[17] Jiang Wen-wei(蒋文伟), Yang Qin(杨 琴), Luo Da(罗 答). CN[P], 101249451A (中国专利), 2008.

[18] Wang J G, Hammer B. Role of Au^+ in supporting and activating Au_7 on TiO_2(110) [J]. *Phys Rev Lett*, 2006, **97**: 136107.

[19] Liu J J, Ge Q F. Hydrogen interaction in Ti-doped $LiBH_4$ for hydrogen storage: a density functional analysis [J]. *J Chem Theory Comput*, 2009, **5**: 3079-3087.

[20] Conte M, Carley A F, Heirene C, *et al*. Hydrochlorination of acetylene using a supported gold catalyst: a study of the reaction mechanism [J]. *J Catal*, 2007, **250**(2): 231-239.

[21] Zhang J L, He Z H, Li W, *et al*. Deactivation mechanism of $AuCl_3$ catalyst in acetylene hydrochlorination reaction: a DFT study [J]. *RSC Adv*, 2012, **2**: 4814-4821.

[22] Badawi M, Paul J F, Cristol S, *et al*. Improving the carbon resistance of Ni-based steam reforming catalyst by alloying with Rh: a computational study coupled with reforming experiments and EXAFS characterization [J]. *J Catal*, 2011, **282**: 155-164.

[23] Becke A D. Density-functional thermochemistry. III. The role of exact exchange [J]. *J Chem Phys*, 1993, **98**: 5648-5652.

[24] Lee C, Yang W T, Parr R G. Development of the colle-salvetti correlation-energy formula into a functional of the electron density [J]. *Phys Rev B*, 1988, **37**: 785-789.

[25] Klippenstein S, Harding L B, Georgievskii Y. On the formation and decomposition of C_7H_8 [J]. *Proc Combust Inst*, 2007, **31**: 221-229.

[26] El-Nahas A M, Mangood A H, Takeuchi H. Thermal decomposition of 2-butanol as a potential nonfossil fuel: a computational study [J]. *J Phys Chem A*, 2011, **115**: 2837-2846.

[27] Zhang H Y, Dai B, Wang X G, *et al*. Hydrochlorination of acetylene to vinyl chloride monomer over bimetallic Au-La/SAC catalysts [J]. *J Ind Eng Chem*, 2012, **18**: 49-54.

[28] Zhang L P, Xia Z H. Mechanisms of oxygen reduction reaction on nitrogen-doped graphene for fuel cells [J]. *J Phys Chem C*, 2011, **115**: 11170-11176.

[29] Xu Long-long(徐龙龙), Wang Xu-gen(王绪根), Zhang Hai-yang(张海洋), *et al*. Application of a novel carbon carrier in acetylene hydrochlorination(一种新型炭载体在乙炔氢氯化反应中的应用) [J]. *Chem Ind Eng Prog*(化工进展), 2011, **30**(3): 536-541.

乙炔氢氯化反应铜系催化剂的反应机理

赵璞君[1], 王富民[1], 蔡旺锋[1], 张金利[1], 张旭斌[1,*]

(天津大学 化工学院, 天津 300072)

摘要: 以电石乙炔法制备氯乙烯的非汞催化反应体系为研究对象, 用量子化学密度泛函理论(DFT)研究了以 Cu 基催化剂为代表的非汞催化剂的反应机理. 模拟了以石墨烯为载体的乙炔氢氯化反应在 Cu 基催化剂作用下的两条反应路径及其过渡态. 将该反应机理应用到不同金属氯化物催化剂中, 通过计算相应的活化自由能和反应速率常数讨论了不同金属氯化物的活性顺序, 与实验结果相比较印证了反应机理的合理性. 讨论了 Cu 基催化剂的失活原因以及在载体中掺杂氮原子或磷原子对反应活性的影响. 为非贵金属无汞催化剂的研究提供了一定的理论指导.

关键词: 乙炔氢氯化反应; Cu 基催化剂; 密度泛函理论; 反应机理; N/P 掺杂